

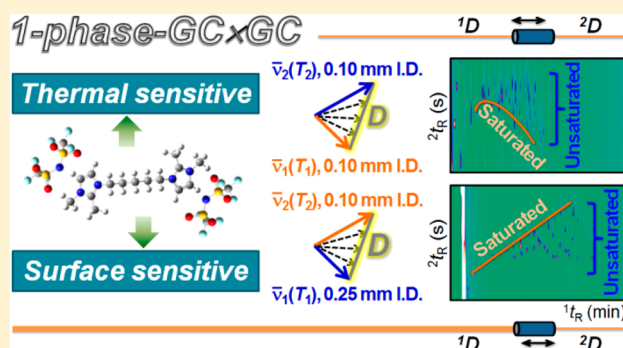
Thermally Sensitive Behavior Explanation for Unusual Orthogonality Observed in Comprehensive Two-Dimensional Gas Chromatography Comprising a Single Ionic Liquid Stationary Phase

Yada Nolvachai, Chadin Kulsing, and Philip J. Marriott*

Australian Centre for Research on Separation Science, School of Chemistry, Monash University, Wellington Road, Clayton, Victoria 3800, Australia

S Supporting Information

ABSTRACT: In this study, a theoretical concept and method to achieve a degree of orthogonality in comprehensive two-dimensional gas chromatography (GC \times GC) for separation of fatty acid methyl esters (FAME) by using a single ionic liquid (IL) stationary phase (1-phase-GC \times GC) were established. The 1-phase system comprises a long IL column and shorter IL column of the same phase before and after the modulation region, operated under temperature-programmed conditions. Initial isothermal experiments employing six commercial IL columns were conducted at different temperatures. On the basis of the temperature-dependent linear solvation energy relationship (LSER) concept, SLB-IL111 exhibited the greatest thermal sensitivity and degree of difference over the tested temperature (T) range, so it was selected for investigation of the 1-phase-GC \times GC mode. With the same temperature program, a significantly high degree of orthogonality was observed for the experiment, varied with column lengths. The switchable separation result, which inverts the retention of saturated and unsaturated FAME on the downstream column (2D), was achieved by varying column diameters and surface thicknesses of the IL-coated layers. These results were explained according to the corresponding LSER principles. Also, the time summation model was applied for the simulation of the observed 1-phase-GC \times GC results.



Ionic liquids (IL) are of interest as stationary phases in gas chromatography (GC); they can exhibit high polarity, possess high thermal stability, and their customizable molecular properties allow the capability to tune the separation result by changing IL molecular structures.^{1–3} The “dual-like property” (the potential to show either nonpolar or polar character) makes IL an even more attractive type of phase.⁴ IL phases may be employed in either one-dimensional (1D) or multidimensional GC methodology, providing additional selectivity compared to conventional phases such as polysiloxane and poly(ethylene glycol).^{5–7} IL columns have been used for the separation of many analyte classes, e.g., hydrocarbons, fatty acid methyl esters (FAME), polychlorinated biphenyls (PCB), or pesticides, in different sample matrixes.^{8–12} Recent investigations involve synthesis of IL-based stimuli-responsive materials where materials undergo a change according to (slight) variation in experimental conditions such as pH, temperature, or presence of specific functional groups providing the benefit of controlled drug delivery or chemical sensing.^{13–16} A key target is to apply the analogous concept of thermal sensitivity of IL in comprehensive two-dimensional gas chromatography (GC \times GC). It will be theoretically and experimentally demonstrated here that a single IL phase possesses thermal- and surface-sensitive behaviors, to achieve

unexpected orthogonality and switchable selectivity in GC \times GC.

GC \times GC has recently attracted the interest of GC users, owing to its potential for improved resolution, most favorably displayed in the analysis of complex mixtures of multi-component samples.^{17–19} This arises from the application of two columns, ideally with sufficient differences in column selectivity (interpreted as different separation mechanisms) toward sample components. The columns are arranged sequentially, with a device that offers a modulation process between the columns^{20,21} to effectively interrupt the passage of solute between the columns—repeatedly collecting or focusing the solute from the upstream column (1D) and then releasing it to the downstream column (2D). This provides a measure of independence to the elution on the two columns, such that unresolved components on 1D may often be well-separated on 2D . Modulation is normally conducted at a period less than the 1D peak width according to the modulation ratio.²⁰ The success and extent of separation on 2D depend on conditions of the experiment, but it is a tenet of GC \times GC that the column

Received: August 12, 2014

Accepted: December 8, 2014

Published: December 8, 2014

phases used in ^1D and ^2D should be different (each column providing independent interaction toward sample components). The two-dimensional separation is then considered to exhibit a measure of orthogonality.

Practically, orthogonality (O) represents the distribution of analyte peaks (of different classes) in 2D chromatograms. In this study, O is scaled from 0 (perfect correlation in the 2D retention plots; zero additional 2D separation information) to 1 (orthogonal; all analytes are well-distributed throughout the 2D chromatogram). Recent progress on the description of peak distribution, evaluation of orthogonality, and column selection in GC \times GC has been reported.^{22,23} O can then be measured by counting the area or bin coverage of analytes in a normalized 2D chromatogram divided by the statistically maximum area covered by the analyte peaks.^{23,24} Correlation between normalized retentions in 1D and 2D separations can then be incorporated into the calculation of O for more accurate description of peak distribution.²³

Maximizing orthogonality in GC \times GC conventionally demands use of two stationary phases of widely differing nature. In some exceptional cases, orthogonality and good separation can be obtained from the use of the same phase in ^1D and ^2D separation.^{25,26} The present study focuses on apparent orthogonality arising from use of a single IL phase (1-phase-GC \times GC). This necessitates the column behaving with suitable thermal sensitivity toward separation of sample components (herein a 37 FAME standard) under temperature-programmed separation.

EXPERIMENTAL SECTION

Chemicals and Materials. A 37-component FAME mixture (47885-U) was obtained from Supelco (Sigma-Aldrich, Bellefonte, PA). GC grade dichloromethane (DCM) was obtained from Merck Co. (Merck KGaA, Darmstadt, Germany). The original FAME mixture (10 000 mg L⁻¹ as total concentration, not individual concentration) was diluted to 250 mg L⁻¹ with DCM.

1DGC Isothermal Experiment. Samples (1 μL , split ratio 500:1) were injected into an Agilent 6850 GC (Mulgrave, Australia) coupled with a flame ionization detector (FID), installed with columns shown in Table S1, Supporting Information. Isovoltality curves of each column were experimentally assessed and were performed by using constant temperature over the range of 150–230 °C, and the data were collected within 2 h. Hydrogen (99.999%) was used as carrier gas at a constant flow rate of 1.5 and 0.3 mL min⁻¹, respectively, for each column. Injector and detector temperatures were 250 and 260 °C. Data were collected at 10 Hz.

GC \times GC Experiment. Samples (1 μL , split ratio 20:1) were injected into an Agilent 7890A GC (Mulgrave, Australia) coupled with an FID and fitted with a longitudinally modulated cryogenic system (LMCS, model 2.02, Chromatography Concepts, Doncaster, VIC, Australia), installed with column sets and flow rates shown in Table S2, Supporting Information. The oven program was initially set at 100 °C (held for 1 min), then increased to 230 °C at a rate of 8 °C min⁻¹, and finally held for 3 min. Temperature ramp variation was also performed at 5 and 15 °C min⁻¹ with similar initial and final temperatures and hold time. Hydrogen (99.999%) was used as carrier gas. Injector and detector temperatures were 250 and 260 °C. Data were collected at 100 Hz.

Modulation period (P_M) was 6 s. Modulation temperature was 20 °C (0–5 min), 30 °C (5–10 min), 50 °C (10–13 min),

60 °C (13–15 min), and 90 °C for the rest of the analysis, except SLB-IL111 (4 m \times 0.10 mm \times 0.08 μm) \times SLB-IL111 (0.825 m \times 0.10 mm \times 0.08 μm) where the modulator temperature was 60 °C. The experiment was performed thrice, with each new segment of ^2D : SLB-IL111. All columns were obtained from Supelco. Agilent ChemStation was used for data acquisition and processing, an in-house application for data conversion, and Fortner Transform (Fortner, Inc., Savoy, IL) for data visualization (2D plots).

RESULTS AND DISCUSSION

Thermal sensitivity of a column to be employed in 1-phase-GC \times GC should ideally result in significant differences between the column segments in their ^1D (temperature-programmed) and ^2D (fast elution \sim isothermal) separation. According to the linear solvation energy relationship (LSER),²² the degree of this difference in phases is captured by the “ D ” parameter as

$$D = |\bar{v}_1 - \bar{v}_2| = [(e_1 - e_2)^2 + (s_1 - s_2)^2 + (a_1 - a_2)^2 + (b_1 - b_2)^2 + (l_1 - l_2)^2]^{1/2} \quad (1)$$

where \bar{v}_i is a five-component vector representing a set of properties of the column segment employed as the i th dimensional separation (in 1-phase-GC \times GC). It is reasonable that disparate columns will have different D values due to column properties changing with temperature in temperature-programmed separation. The five components of \bar{v}_i derive from stationary phase descriptors representing interaction properties contributed from the stationary phase. These interactions are lone pair electrons and π -electrons (e_i), dipole–dipole or dipole–induced dipole (s_i), hydrogen-bond basicity with acid analytes (a_i), hydrogen-bond acidity with basic analytes (b_i), and dispersity/cavity formation (l_i). The subscript i represents the property of the column segments for ^1D ($i = 1$) and ^2D ($i = 2$) separations, respectively.

Better orthogonality (O value closer to unity) is expected when the single column provides a larger D value between the two segments under a certain temperature program profile. All parameters in eq 1 are functions of temperature (T). The T -dependent IL descriptors of each IL column, SLB-IL59, 61, 76, 82, 100, 111 (0.10 mm i.d.) or 111 (0.25 mm i.d.), were experimentally obtained by fitting experimental results for 1D isothermal separations of 37 FAME at different temperatures to the LSER equation (see eq S1 and Figure S1, Supporting Information for the fitting result). Note that the molecular structures and properties of the studied IL phases were previously reported.² The relationship between all IL descriptors and T , $x_i(T)$, where x is e , s , a , b , l , or c , was well-fitted to polynomial equations up to power 6 (see Figure 1, also see eq S2 and Table S3, Supporting Information for the fitting result and the corresponding coefficient values of each term in the polynomial equations). Note that the IL descriptors calculated in this study are more effectively applicable for FAME analytes. More general IL descriptor values (for any analytes) have been reported.²⁷

Since different analytes arrive at the detector at different times, each analyte interacts with a single column with different T histories for their ^1D and ^2D separations in a T -programmed 1-phase-GC \times GC analysis. The T program in all cases was selected to be at 100 °C for 1 min, then from 100 to 230 °C (8 °C min⁻¹) during which all analytes elute; modulation period was fixed at 0.1 min (6 s). For each analyte elution, the ^1D

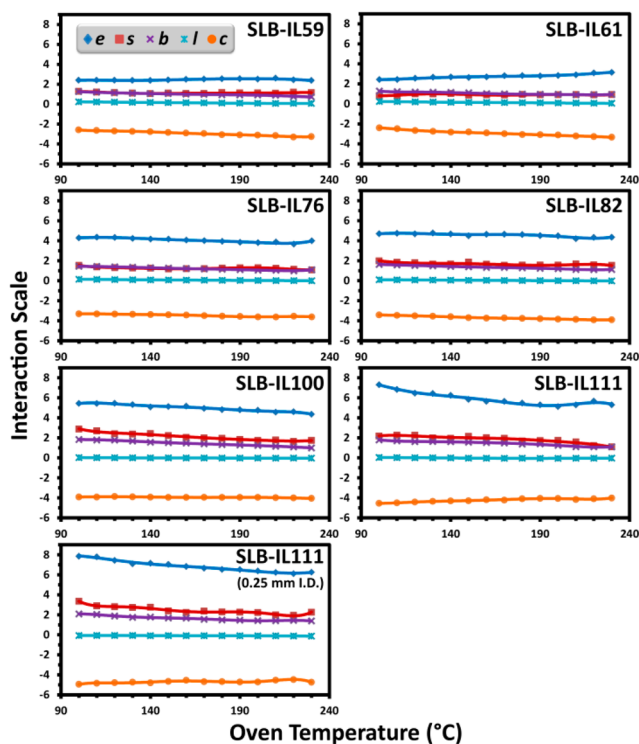


Figure 1. Calculated LSER descriptors value, x (being e , s , a , b , l , and c), at different temperatures (represented by dots) obtained from curve fitting with 1DGC isothermal separation according to Figure S1, Supporting Information. Lines represent corresponding curve fitting according to eq S2, Supporting Information.

column segment experienced gradient temperature while the 2D column segment was assumed to a first approximation to be isothermal. For example, an analyte with elution time of 10 min will have a T -variable interaction with the 1D column segment for $9.95 (\pm 0.05)$ min, and an isothermal interaction with the 2D column segment for $0.05 (\pm 0.05)$ min, regardless of the presence of wraparound. This analyte will experience a gradient T from 100.00 to $179.60 (\pm 0.40)$ °C on 1D , and the 2D column segment experiences a constant temperature at $179.60 (\pm 0.40)$ °C. The calculation of the related IL descriptors for each column segment should be correspondingly adjusted. The x_2 values at different temperatures (also different analyte retention time) were directly obtained from the fitted polynomial equations in 1DGC experiments, while the x_1 values in this study are taken as the average values of IL descriptors, x_{ave} (x being e , s , a , b , l , or c), for this segment over the T range. The x_{ave} with the temperature program here were calculated from the polynomial function of each IL descriptor as a function of T (°C), denoted by $x(T)$, as

$$x_1 = x_{ave}(T_R) = x(100) \quad \text{at } T_R = 100 \text{ °C}$$

$$= \frac{x(100) + \frac{1}{\gamma} \int_{T=100}^{T=T_R} x(T) dT}{t_R} \quad \text{at } T_R > 100 \text{ °C} \quad (2)$$

where γ , t_R , and T_R are program rate (°C min $^{-1}$), analyte retention time (min), and T (°C) at t_R , respectively. $T_R = 100$ °C when $t_R = 0$ –1 min, and $T_R = 100 + \gamma(t_R - 1)$ when $t_R > 1$ min. When $t_R > 1$ min, eq 2 is taken as the weighted average of average descriptor values during the period when the temperature was kept constant at 100 °C and then ramped

from 100 to T_R . Due to x_1 and x_2 varying with t_R , the D value for each column employed in 1-phase-GC \times GC depends on t_R . All calculated x_1 , x_2 , and D values at different t_R for each studied IL column are shown in Tables S4–S9, Supporting Information.

The plot of D value versus t_R is thus a meaningful general approach for selection of a column to be employed in the 1-phase-GC \times GC experiment. Such plots are shown in Figure 2.

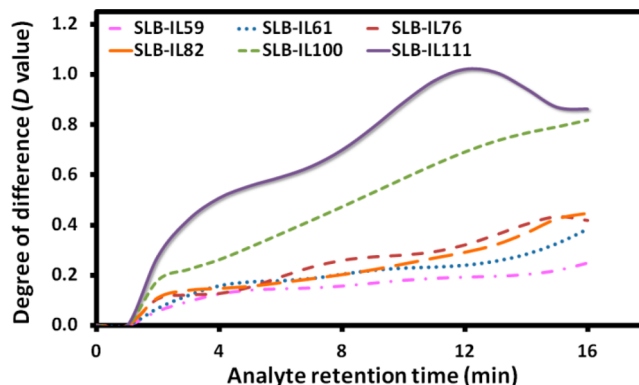


Figure 2. Plot between degree of difference (D value) and analyte retention employing different IL columns (all with 0.10 mm i.d.) in 1-phase-GC \times GC mode. The temperature in all cases was selected to be at 100 °C for 1 min, then 100–230 °C (8 °C min $^{-1}$).

SLB-IL111 (1,5-di(2,3-dimethylimidazolium)pentane bis-(trifluoromethylsulfonyl)imide) appeared to have the most suitable thermal sensitivity behavior with the largest D values within the studied time frame, to exhibit differences between 1D and 2D selectivity.

Since the D value is just a scalar measure based on overall LSER vectors, further information for the difference of each LSER value between the two segments ($\Delta x = x_2 - x_1$) was achieved (Tables S4–S9, Supporting Information). The plots of different Δx versus t_R (Figure S2, Supporting Information) reveal that SLB-IL111 descriptors had great sensitivity toward the t_R as reflected in the prevailing T . This column, expected to provide the best orthogonality in the 1-phase-GC \times GC experiment, was thus selected for further investigation. The experimental results for SLB-IL111 are shown in Figure 3A revealing high degree of orthogonality (O) calculated using the described method²³ for FAME of $\geq C_{13}$ (eqs S19–S21 and Figure S3, Supporting Information).

For increased 2D retention, analytes should elute at lower 1t_R ; retention exponentially decreases with higher T .² This concept was proved herein by varying length of the 1D column segment. Decreasing length resulted in earlier elution time of FAME and lower elution T , increasing 2D retention. This behavior is illustrated in Figure S4, parts A and B, Supporting Information. Decreased peak coverage in 1-phase-GC \times GC results was observed when a longer 1D segment was used (at fixed 2D segment length).

The effect of wraparound, which could affect the interpretation of orthogonality observed in Figure 3A, was investigated on a single SLB-IL111 column passed through the cryogenic modulator (0.1 mm i.d. on both 1D and 2D). The P_M setting was increased to 30 s, with all other conditions being the same as that in Figure 3A. The result revealed that a measure of orthogonality interpreted as a lower polarity–higher polarity phase combination was still observed even without the presence

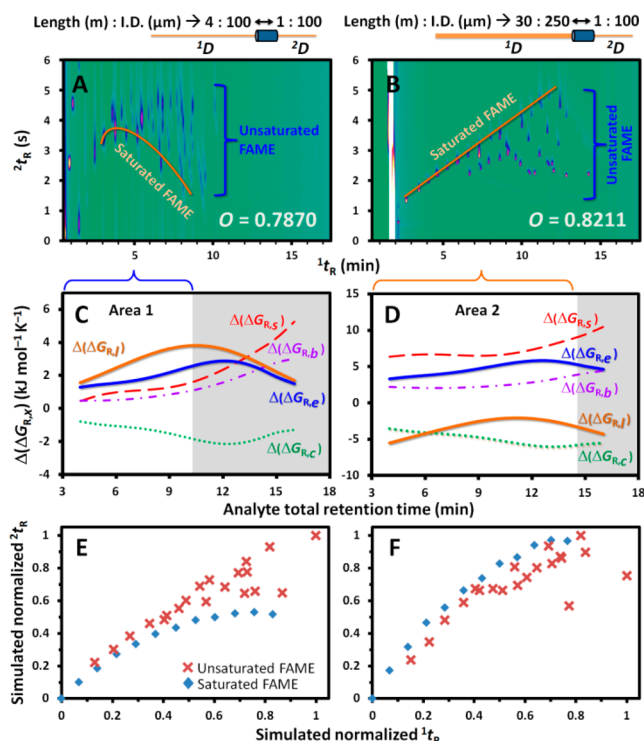


Figure 3. Switchable GC \times GC results by variation of length and i.d. of the SLB-IL111 segment used in 1D separation, (A) 4 m \times 0.10 mm i.d. \times 0.08 μm d_f and (B) 30 m \times 0.25 mm i.d. \times 0.08 μm d_f , with the same 2D segment of SLB-IL111 (0.825 m \times 0.10 mm i.d. \times 0.08 μm d_f). The plots of different $\Delta(\Delta G_{R,x})$ vs analyte elution time for the column sets employed in panels A and B are shown in panels C and D, respectively, for the 37 FAME standard. The temperature program is the same as that in Figure 2. The corresponding simulation results are shown in panels E and F (simulation parameters as shown in Table S11, Supporting Information).

of the wraparound (Figure S5, Supporting Information). This observation confirms that orthogonality of phase properties was caused by the temperature-dependent selectivity of IL columns toward different FAME as previously reported for the conventional non-IL columns applied in 1DGC.²⁸

Interestingly, with SLB-IL111 employed in both 1D and 2D separations, variation of column i.d. provided a switched elution pattern of FAME. Unsaturated FAME elute later in 2D (Figure 3A) interpreted as 1D being of lower polarity and 2D being of more polar-like character; saturated FAME elute later in 2D (Figure 3B) interpreted as 1D being more polar and 2D being of lower polar-like character. This observation was caused by the dependence of column property on temperature and, presumably, the manner that column i.d. affects interplay between adsorption and partition mechanisms, carrier flow, and elution T . The trends of variation in LSER descriptors with temperature for SLB-IL111 with different i.d. (0.10 and 0.25 mm) and film thicknesses (0.2 and 0.08 μm) were similar. However, their magnitudes are different as shown in Figure 1. Despite being the same phase, this magnitude difference could result from surface adsorption which is affected more strongly for the smaller i.d. column with the thinner film (higher surface to volume ratio). The smaller i.d. SLB-IL111 has larger l and c values with smaller e , s , and b values (Figure 1). Our result is in agreement with the previous report of decreasing phase “polarity” (analogous to the decreasing e and s values herein)

by using thinner coated layer (increasing surface to volume ratio) of cyanopropyl/phenyl polysiloxane phase (SP-2380).²⁹

The difference of Gibbs energies related to the retention of FAME between the 1D and 2D column segments, contributed from different types of LSER-based interactions noted as $\Delta(\Delta G_{R,x})$ (x being e , s , a , b , l , or c), were calculated (eqs S3–S10, Supporting Information) from the corresponding data in Tables S9 and S10, Supporting Information. The corresponding values of $\Delta(\Delta G_{R,x})$ were plotted against elution time of a representative FAME (an analyte having average descriptor values of all FAME in this study) in Figure 3, parts C and D (for the experiment in Figure 3, parts A and B, respectively). The most critical parameters are $\Delta(\Delta G_{R,e})$ and $\Delta(\Delta G_{R,l})$ being the energy related to the electron pair and cavity formation/dispersion interactions in the 2D column, respectively. The negative and positive values of these parameters correspond to the energies released (additional interaction in 2D) and gained (decreasing interaction in 2D), respectively, by the system when a mole of the representative FAME moved from the 1D to 2D column segment. For FAME with the same carbon number, retention of unsaturated FAME was influenced more strongly by the electron pair interaction, while saturated FAME retention was more sensitive to cavity formation/dispersion interaction. $\Delta(\Delta G_{R,e})$ and $\Delta(\Delta G_{R,l})$ thus impact the observed switchable trend. The other $\Delta G_{R,x}$ values approximately equally affect 2D retention of all FAME, so insignificantly affect the trend of switching retentions.

The ranges of times during which all analytes elute in Figure 3, parts A and B, correspond to the unshaded regions area 1 and area 2 in Figure 3, parts C and D, respectively. The same 1D to 2D column set occupied the period when $\Delta(\Delta G_{R,l})$ was more positive than $\Delta(\Delta G_{R,e})$ (area 1). This behavior corresponded to the trend of 2D retention of unsaturated FAME located above the position of saturated FAME in Figure 3A, especially at higher temperature. On the other hand, for the separation in Figure 3B, the time when $\Delta(\Delta G_{R,l})$ was more negative than $\Delta(\Delta G_{R,e})$ (area 2) caused switching of 2D retention time of saturated FAME to now be greater.

Beside discussion based on a representative FAME, further insight is achieved by taking into account each FAME t_R which can be predicted by using a time summation model following the relationships in eqs 3 and 4.³⁰

$$L_i \leq \sum_{j=0}^n \Delta x_j = \sum_{j=0}^n \frac{u_j}{1 + k_j} \Delta t \quad (3)$$

$$t_{R,i} = n \Delta t \quad (4)$$

where j is step number in the calculation and L_i is capillary segment length employed as the i th dimensional separation. Δx_j is the length at step j (cm), and Δt is the time step of calculation (0.0001 min in this study). n is the minimum number of steps satisfying eq 3. u_j and k_j are velocity of the carrier gas and analyte retention at step j , eqs S11–S15, Supporting Information. Equations 3 and 4 were applied for simulation of the 1-phase-GC \times GC results in Figure 3 using script developed with Microsoft Visual Basic for Applications in Microsoft Excel 2010. The simulation trends in Figure 3, parts E and F, match quite well to the experimentally observed switchable trends in Figure 3, parts A and B.

Although the general switchable trend in Figure 3 can be simulated, the slope of the simulated 2t_R versus 1t_R in Figure 3E is positive which did not match well with the experimental

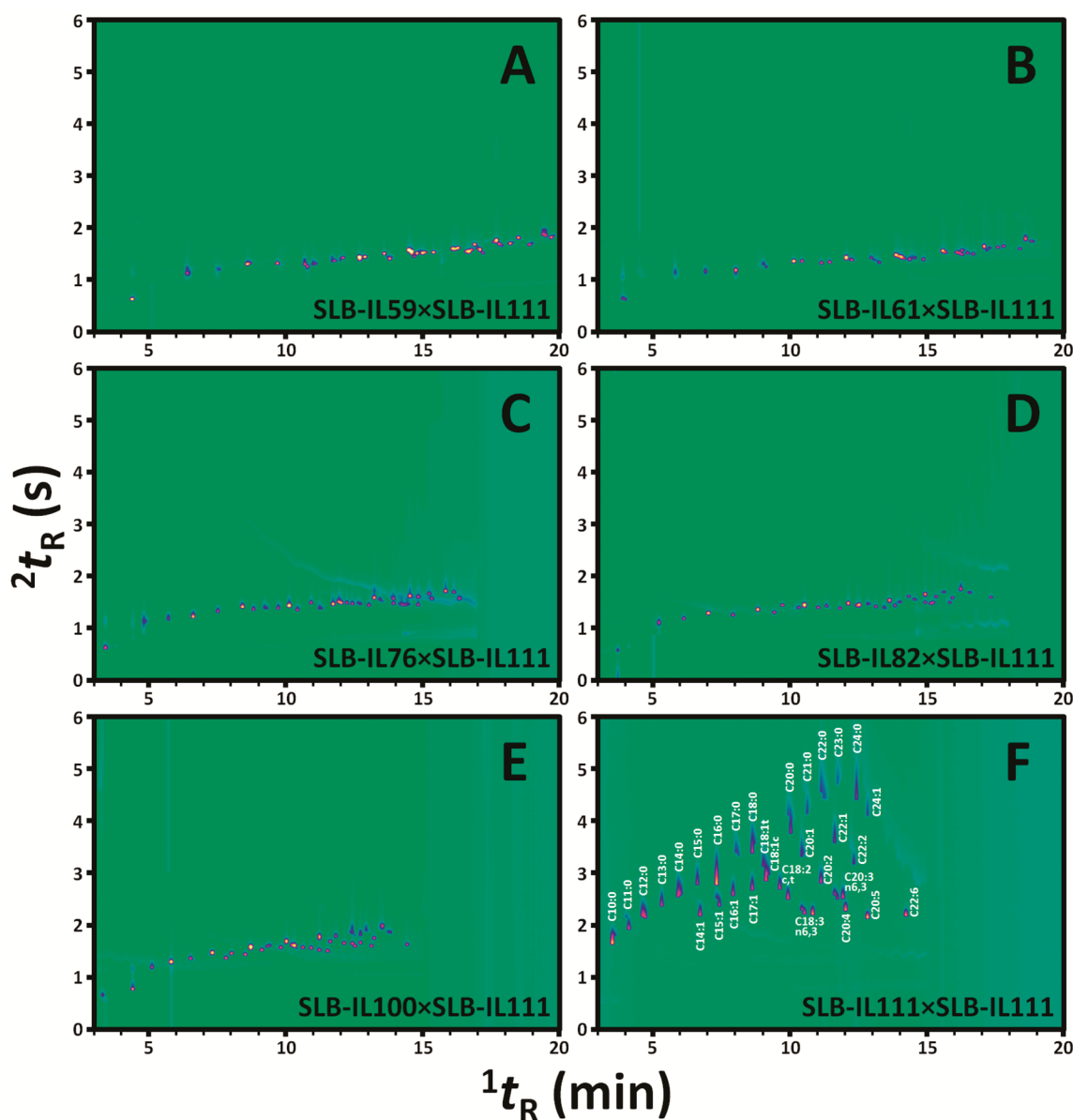


Figure 4. Contour plots of the 37 FAME obtained by variation of 1D stationary phase (all 30 m \times 0.25 mm i.d. \times 0.20 μm d_f) using SLB-IL59, 61, 76, 82, and 100 and 111, panels A–F, respectively. All 2D SLB-IL111 columns were 0.825 m \times 0.10 mm i.d. \times 0.08 μm d_f . The temperature program is the same as that in Figure 2.

negative slope at higher 1t_R observed in Figure 3A. We assume this to be due to the unavoidable deviation of the pressure values reported by the instrument (which is operated in constant flow mode) from the actual values, which are required as input values for the simulation program. Change in the pressure values could thus result in a better simulation as shown in Figure S6, Supporting Information, to better match the experiment shown in Figure 3A.

SLB-IL111 phase was installed as the 2D column. Contrary to expectation, considerably better separation resulted when SLB-IL111 was also used as the 1D column (see Figure 4). Conventionally, we would expect the most disparate column set—SLB-IL59 \times SLB-IL111—to give the most “orthogonal” arrangement, as a lower-polarity–higher-polarity combination. The SLB-IL111 \times SLB-IL111 result is in our experience unprecedented. It is a striking indication of the potential of 1-phase-GC \times GC mode in practical analytical applications.

The effect of temperature gradient variation was also investigated for the SLB-IL111 (0.25 mm i.d.) \times SLB-IL111 (0.10 mm i.d.). Compared with the 8 $^\circ\text{C min}^{-1}$ ramp (Figure 4F), the slower ramp rate (5 $^\circ\text{C min}^{-1}$) resulted in the peaks being further spread in both 1D and 2D , with some wraparound observed in the result shown in Figure 5A. A more compact distribution of peaks was observed with the faster ramp rate (15 $^\circ\text{C min}^{-1}$, Figure 5B).

Another interesting point is that a similar elution behavior (unsaturated FAME having lower 2t_R than the corresponding saturated FAME as shown in Figure 4F and Figure 5, parts A and B) was previously observed by Delmonte et al.,²⁶ where SLB-IL111 (200 m \times 0.25 mm i.d. \times 0.20 μm d_f) was also coupled with SLB-IL111 (2.75 m \times 0.10 mm i.d. \times 0.08 μm d_f). Since all unsaturated FAME were reduced to their corresponding saturated FAME through the use of a Pd catalyst-coated capillary located between the junction of the two SLB-IL111 columns, the 2D column was only employed to separate the

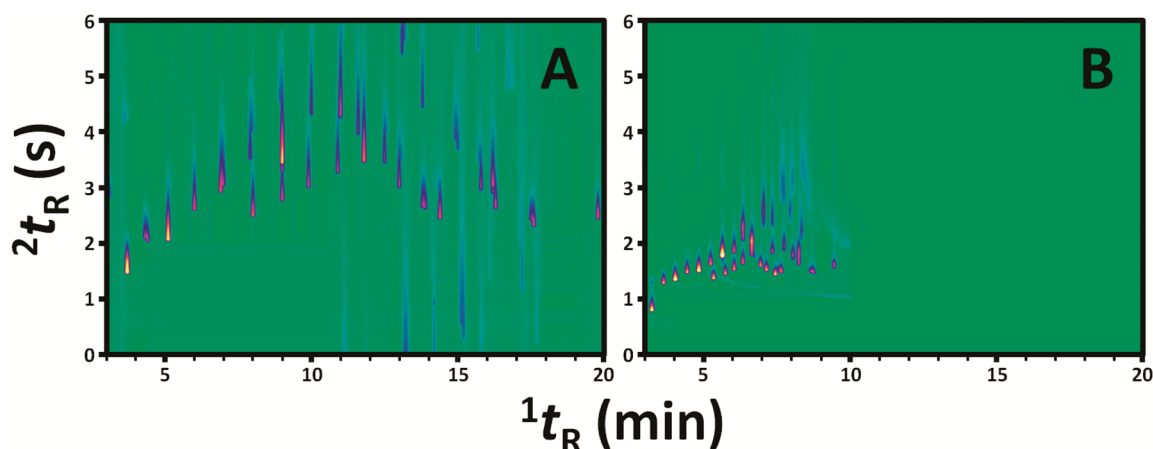


Figure 5. Contour plots of the 37 FAME obtained by using SLB-IL111 ($30 \text{ m} \times 0.25 \text{ mm i.d.} \times 0.20 \text{ } \mu\text{m } d_i$) \times SLB-IL111 ($0.825 \text{ m} \times 0.10 \text{ mm i.d.} \times 0.08 \text{ } \mu\text{m } d_i$) with temperature ramping rate of (A) 5 and (B) $15 \text{ } ^\circ\text{C min}^{-1}$.

homologues of saturated FAME; presumably, any ^2D column could be used for this purpose. It should also be noted that the 2t_R values were observed to be higher in our study due to the slower carrier gas flow rate used in this study and isothermal conditions. The flow rate ranges used in the present study and those reported by Delmonte et al. are 144–203 and 483–588 kPa, respectively.

CONCLUSION

The unusual observation of an apparent degree of orthogonality obtained from a single IL column has led to theoretical concepts and methods for column selection to express orthogonality in the T -programmed 1-phase-GC \times GC experiment. As a generality, we interpret that a stationary phase exhibiting such behavior should be one that shows a high degree of difference in D value as a function of temperature, over the elution time frame of separated analytes in a 1DGC experiment. SLB-IL111 provided good orthogonality for FAME separation due to its suitable thermal and surface sensitive behaviors, resulting in a significantly high degree of difference between the two (^1D and ^2D) column segments, both comprising the same IL phase. However, high D values should be mostly obtained at low temperature since overall retention of analytes exponentially decreased at higher temperature. A further outcome of interpretation of GC \times GC employing a single IL stationary phase was demonstrated with the tunable separation pattern, achieved simply by varying the ^1D column dimensions; this resulted in the GC \times GC result being switched, to swap relative elution orders on the ^2D column, supported by the simulation based on the time summation model. A situation when the 1-phase-GC \times GC mode provided better separation compared to the other IL column sets was also experimentally illustrated. However, the advantages of a 1-phase-GC \times GC over a conventional GC \times GC method are not clear; the observation of the 1-phase approach to GC \times GC is expected to be an anomaly, and searching for best orthogonality employing 2-phase-GC \times GC is still valid. The thermal and surface sensitivity of the IL phase shown here offers a further complementary mechanism to be employed in higher dimensional GC, such as 3D- or even 4DGC where maximizing available separation mechanisms may be important. This study introduces 1-phase-GC \times GC as a new approach for IL phase application as well as contributes to the concept of orthogonality in GC \times GC.

ASSOCIATED CONTENT

Supporting Information

Detailed calculation and computation method. This material is available free of charge via the Internet at <http://pubs.acs.org>.

AUTHOR INFORMATION

Corresponding Author

*E-mail: philip.marriott@monash.edu.

Notes

The authors declare no competing financial interest.

ACKNOWLEDGMENTS

Y.N. acknowledges the Monash University Institute of Graduate Research, Monash School of Chemistry and Faculty of Science for a scholarship. We acknowledge funding from the ARC Discovery and Linkage program Grants DP130100217 and LP130100048. P.J.M. acknowledges ARC funding for a Discovery Outstanding Researcher Award. The authors thank Supelco (Sigma-Aldrich) for provision of IL columns.

REFERENCES

- (1) Hantao, L. W.; Najafi, A.; Zhang, C.; Augusto, F.; Anderson, J. L. *Anal. Chem.* **2014**, *86*, 3717–3721.
- (2) Kulsing, C.; Nolvachai, Y.; Zeng, A. X.; Chin, S.-T.; Mitrevski, B.; Marriott, P. J. *ChemPlusChem* **2014**, *79*, 790–797.
- (3) Payagala, T.; Zhang, Y.; Wanigasekara, E.; Huang, K.; Breitbach, Z. S.; Sharma, P. S.; Sidisky, L. M.; Armstrong, D. W. *Anal. Chem.* **2009**, *81*, 160–173.
- (4) Anderson, J. L.; Ding, J.; Welton, T.; Armstrong, D. W. *J. Am. Chem. Soc.* **2002**, *124*, 14247–14254.
- (5) Seeley, J. V.; Seeley, S. K.; Libby, E. K.; Breitbach, Z. S.; Armstrong, D. W. *Anal. Bioanal. Chem.* **2008**, *390*, 323–332.
- (6) Reid, V. R.; Crank, J. A.; Armstrong, D. W.; Synovec, R. E. *J. Sep. Sci.* **2008**, *31*, 3429–3436.
- (7) Siegler, W. C.; Crank, J. A.; Armstrong, D. W.; Synovec, R. E. *J. Chromatogr. A* **2010**, *1217*, 3144–3149.
- (8) Poole, C. F.; Lenca, N. *J. Chromatogr. A* **2014**, *1357*, 87–109.
- (9) Zeng, A. X.; Chin, S. T.; Nolvachai, Y.; Kulsing, C.; Sidisky, L. M.; Marriott, P. J. *Anal. Chim. Acta* **2013**, *803*, 166–173.
- (10) Nosheen, A.; Mitrevski, B.; Bano, A.; Marriott, P. J. *J. Chromatogr. A* **2013**, *1312*, 118–123.
- (11) Ragonese, C.; Sciarrone, D.; Tranchida, P. Q.; Dugo, P.; Mondello, L. *J. Chromatogr. A* **2012**, *1255*, 130–144.
- (12) Zapadlo, M.; Krupčík, J.; Májek, P.; Armstrong, D. W.; Sandra, P. J. *J. Chromatogr. A* **2010**, *1217*, 5859–5867.

- (13) Sui, X.; Hempenius, M. A.; Vancso, G. J. *J. Am. Chem. Soc.* **2012**, *134*, 4023–4025.
- (14) Feng, X.; Sui, X.; Hempenius, M. A.; Vancso, G. J. *J. Am. Chem. Soc.* **2014**, *136*, 7865–7868.
- (15) Bai, Z.; Lodge, T. P. *J. Am. Chem. Soc.* **2010**, *132*, 16265–16270.
- (16) Kohno, Y.; Ohno, H. *Phys. Chem. Chem. Phys.* **2012**, *14*, 5063–5070.
- (17) Marriott, P. J.; Chin, S. T.; Maikhunthod, B.; Schmarr, H. G.; Bieri, S. *TrAC, Trends Anal. Chem.* **2012**, *34*, 1–20.
- (18) Chin, S.-T.; Marriott, P. J. *Chem. Commun.* **2014**, *50*, 8819–8833.
- (19) Meinert, C.; Meierhenrich, U. J. *Angew. Chem., Int. Ed.* **2012**, *51*, 10460–10470.
- (20) Khummueng, W.; Harynuk, J.; Marriott, P. J. *Anal. Chem.* **2006**, *78*, 4578–4587.
- (21) Adahchour, M.; Beens, J.; Vreuls, R. J. J.; Brinkman, U. A. T. *TrAC, Trends Anal. Chem.* **2006**, *25*, 540–553.
- (22) Poole, S. K.; Poole, C. F. *J. Sep. Sci.* **2008**, *31*, 1118–1123.
- (23) Zeng, Z. D.; Hugel, H. M.; Marriott, P. J. *Anal. Chem.* **2013**, *85*, 6356–6363.
- (24) Davis, J. M. *J. Sep. Sci.* **2005**, *28*, 347–359.
- (25) Chifuntwe, C.; Zhu, F.; Huegel, H.; Marriott, P. J. *J. Chromatogr. A* **2010**, *1217*, 1114–1125.
- (26) Delmonte, P.; Fardin-Kia, A. R.; Rader, J. I. *Anal. Chem.* **2013**, *85*, 1517–1524.
- (27) Rodríguez-Sánchez, S.; Galindo-Iranzo, P.; Soria, A. C.; Sanz, M. L.; Quintanilla-López, J. E.; Lebrón-Aguilar, R. *J. Chromatogr. A* **2014**, *1326*, 96–102.
- (28) Sidisky, L. M.; Ridley, H. J. *J. High Resolut. Chromatogr.* **1991**, *14*, 191–195.
- (29) Sidisky, L. M.; Rijks, J. A. *J. Microcolumn Sep.* **1992**, *4*, 129–133.
- (30) McGinitie, T. M.; Harynuk, J. J. *J. Chromatogr. A* **2012**, *1255*, 184–189.